UNIVERSITAT POLITÈCNICA DE CATALUNYA
BARCELONATECH

POSITION ESTIMATION FOR IR-UWB SYSTEMS USING COMPRESSIVE SENSING

A DegreeThesis

Submitted to the Faculty of the

EscolaTècnicad'Enginyeria de Telecomunicació de Barcelona

UniversitatPolitècnica de Catalunya

by

Genís Floriach Pigem

In partial fulfilment

of the requirements for the degree in

Science and Telecommunications Technologies ENGINEERING

Advisor: Montse Nájar Marton

Co-advisor: Eva Lagunas Targarona

Barcelona, June 2014

Abstract

Ultra-Wideband (UWB) technology, thanks to its high time resolution, arises as an excellent candidate to provide accurate positioning information in cluttered environments. However, the dense multipath and strong attenuation of the Line-of-Sight (LOS) present in UWB channels poses additional challenges to positioning algorithms. Therefore, in this thesis we have mainly focused on designing an algorithm robust to these problems. Specifically, we have developed two different techniques based on a frequency domain receiver. The first one is based on a Direct Position Estimation (DPE) approach, that is, estimating the position directly from the observed signals, while the second is based on “soft” two-steps approach, where more than one estimated Time of Arrival (TOA) is estimated on each anchor, then in the second stage the best estimators are used to find the position. Simulation results proof the accuracy of the proposed algorithms.

Besides, the proposed methods have also been tested while using Compressive Sensing (CS). CS is a new sensing paradigm that allows compressing signals while they are being sampled, thus it allows to sample at a lower rather than the Nyquist limit.

Resum

La tecnologia Ultra-Wideband (UWB), gràcies a la seva alta resolució temporal, es presenta com un candidat ideal per proporcionar informació de la posició precisa en ambients molt densos. Tanmateix, la gran concentració de propagació multi camí, així com la forta atenuació del camí de visió directa (LOS) característica del canals UWB comporta grans dificultats a l'hora d'estimar la posició. Per aquesta raó, en aquesta tesis ens hem centrat principalment en dissenyar algoritmes robusts a la problemàtica que presenten els canals UWB. Concretament, hem desenvolupat dues tècniques basades en un receptor en el domini freqüencial. La primera està basada en una estimació directa de la posició (DPE) a partir dels senyals rebuts, mentre que la segona està basada en una estimació en dues etapes però amb la diferència que en la primera etapa es proporcionen diversos estimadors del temps de vol (TOA) i en la segona es seleccionen els millors estimadors per trobar la posició. Els resultats de les simulacions demostren la precisió dels algoritmes proposats.

A més a més, els mètodes proposats també s'han provat fent servir Compressive Sensing (CS). CS és un nou paradigma en la teoria del mostreig que permet comprimir una senyal mentre s'està mostrejant, permetent així mostrejar per sota del límit de Nyquist.

Resumen

La tecnología Ultra-Wideband (UWB), gracias a su alta resolución temporal, se presenta como un candidato ideal per proporcionar información de la posición precisa en ambientes muy densos. Sin embargo, la gran concentración de propagación multi camino, así como la fuerte atenuación del camino de visión directa (LOS) característica de los canales UWB conlleva grandes dificultades a la hora de estimar la posición. Por esta razón, en esta tesis nos hemos centrado principalmente en diseñar algoritmos robustos a la problemática que presenten los canales UWB. Concretamente, hemos desarrollado dos técnicas basadas en un receptor en el dominio de la frecuencia. La primera está basada en una estimación directa de la posición (DPE) a partir de las señales recibidas, mientras que la segunda está basada en una estimación en dos etapas pero con la diferencia que en la primera etapa se proporcionen diversos estimadores del tiempo de vuelo (TOA) y en la segunda se seleccionen los mejores estimadores para estimar la posición. Los resultados de les simulaciones demuestran la precisión del los algoritmos propuestos.

Además, los métodos propuestos también se han probado utilizando Compressive Sensing (CS). El CS es un nuevo paradigma en la teoría del muestreo que permite comprimir una señal al mismo tiempo que se está muestreando, permitiendo así muestrear per debajo del límite de Nyquist.

Revision history and approval record

Revision	Date	Purpose
0	07/06/2016	Document creation
1	28/06/2016	Document revision

DOCUMENT DISTRIBUTION LIST

Name	e-mail
Genís Floriach Pigem	gfloriach94@gmail.com
Montse Nájar Marton	montse.najar@upc.edu
Eva Lagunas Targarona	eva.lagunas@uni.lu

Written by:		Reviewed and approved by:	
Date	26/06/2016	Date	28/06/2016
Name	Genís Floriach Pigem	Name	Montse Nájar Marton
Position	Project Author	Position	Project Supervisor

Table of contents

1. List of Figures

2. List of Tables:

3. Introduction

In the recent decade, during which global positioning system (GPS) receivers have been successively integrated in more and more devices dedicated to the consumer market, the nearly continuous knowledge of own location has become an almost obvious thing for many of us. However, while GPS works successfully in open space, it presents significant problems in cluttered environments (inside buildings, in urban canyons…) where the actual accuracy is limited to some tens and several hundreds of meters, which is significantly lower than that achievable in open space (in order of a few meters). In many cases the GPS signal is too weak to penetrate inside the building and even if it does the presence of walls, obstructions and obstacles cause severe multipath propagation which makes it extremely problematic to accurately estimate the Time of Arrival (TOA) of the direct path.

Nevertheless, even if GPS worked as well as it does in open space environments, the GPS accuracy would not be high enough for many indoor positioning applications where the required accuracy is at least one order of magnitude higher than what the current GPS could offer. Ultra-Wideband (UWB) technology arises as an ideal candidate to provide positioning information in such cluttered environments. The use of extremely short time domain pulses with several GHz of bandwidth offers a high time resolution which allows resolving the multipath components as well as penetrating obstacles.

Although UWB technologies present very promising features for positioning, there are still several challenges that need to be addressed. In indoor UWB channels, the dense multipath poses additional challenges to positioning. Moreover, the LOS may be considerably attenuated with respect to other multipath delays.

Apart from that, the extremely large bandwidth of UWB signals requires a very high sampling rate which may be costly or even impractical. Therefore, it is desirable to design positioning algorithms that can provide high accuracy while sampling at low-rate. A new sampling paradigm called Compressive Sensing (CS) arises as promising solution to overcome this constraint.

That being said, in this project we will focus on designing positioning algorithms robust to the harsh UWB channels. This project has been developed along another student, Ricard Garcia, who has focused on applying compressive sensing techniques to the UWB positioning problem. Then, the presented solutions in this work have also been tested while applying compressive sensing.

4. State of the art of the technology used or applied in this thesis:

In this section, we will make a brief review of the UWB technology as well as the current position estimation techniques developed. Furthermore, we will introduce compressive sensing and its applications to positioning.

1.2 Ultra-Wideband technology:

According to the U.S Federal Communications Commission (FCC) any wireless communications technology that produces signals with an absolute bandwidth of at least 500MHz or a fractional bandwidth greater than 0.2 can be considered as UWB. The absolute bandwidth is obtained as the difference between the upper frequency f_H of the -10dB emission point and the lower frequency f_L of the -10dB emission point. On the other hand, the fractional can be determined as:

$$B_f = 2 \cdot \frac{f_H - f_L}{f_H + f_L}$$

But in these case f_H and f_L are the upper and lower -3dB emission point, respectively.

One of the major limitations of UWB to enter the commercial market was the legislation. As UWB signals occupy a very large portion in the spectrum, they need to coexist with the conventional transmission systems without causing significant interference and performance degradation perceptible by their users. After several years of work, the FCC assigned a big portion of spectrum for license-free usage in 2002. Four years later, the Electronic Communications Committee (ECC) followed their lead. However, these regulations strictly defined the allowed transmitted average power and the frequency profile, making it possible for UWB devices to be operated as an overlay system. Specifically, the transmitted average power spectral density must not exceed -41.3dBm/MHz over the frequency band from 3.1 to 10.6 GHz, and it must be even lower outside this band. Fig. 1 shows the current proposal for the FCC masks for data communication applications for indoor and outdoor use. After the legalization of UWB signals, a considerable amount of effort has been put into the development of UWB systems.

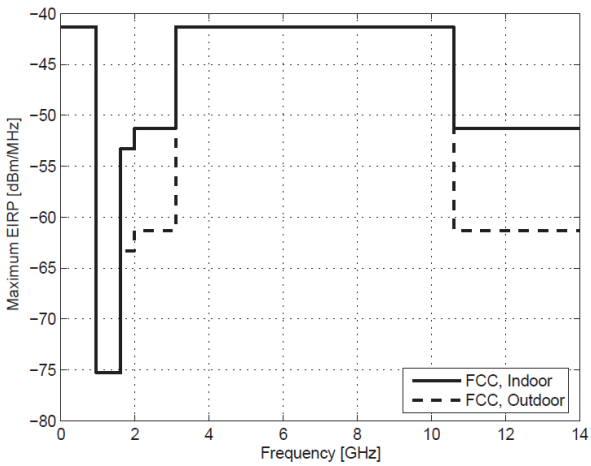

Fig. 1 UWB radiation mask defined by FCC

1.2.1 Characteristics of UWB

A possible technique for implementing UWB is impulse radio (IR), which is based on transmitting extremely short (in the order of nanoseconds) and low power pulses with a low duty cycle. In an IR-UWB communications system, a number of UWB pulses are transmitted per symbol and information is usually encoded in the position of theses pulses in time (PPM, pulse position modulation) or in the polarities of the pulses (PAM, Pulse amplitude modulation) (Fig. 2).

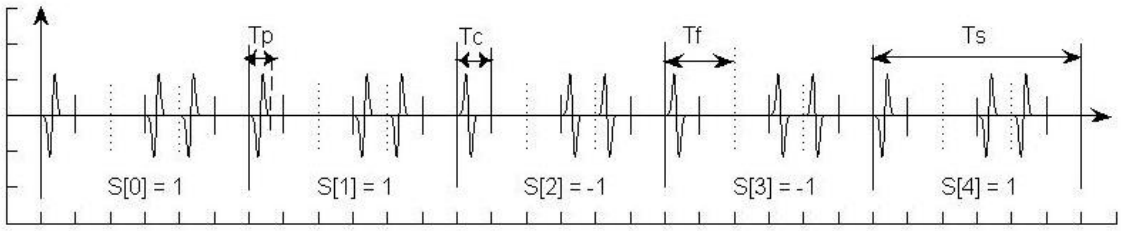

Fig. 2 UWB signal consisting of short duration pulses with a low duty cycle, where Tp is the duration of the pulse, Tc is the chip duration, Tf represents the pulse repetition interval or time of frame and Ts is the duration of the symbol.

Large bandwidth of UWB signals brings many advantages for positioning, communications and radar applications. In particular:

- Penetration through obstacles
- High time domain resolution
- Noise-like spectrum
- Low cost, low complexity and low power transmission
- High-speed data transmission

UWB signals show low material penetration losses thanks to the fact that its large bandwidth includes both low and high frequency components. This large spectrum also results in high time resolution, which improves the ranging accuracy and it provides robustness against multipath as well. These are the main features that make UWB systems suitable for indoor positioning.

Due to the low energy density, the pseudo-random *(PR)* characteristics of the signal and the fact that the energy is spread out over a very large bandwidth, the UWB signal is noise-like, therefore the probability of detection/interception is very low, which makes it suitable for military applications. Thanks to these features, UWB systems can operate on occupied bands without causing significant interference.

The low complexity and low cost of UWB comes from the essentially baseband nature of the signal transmission. UWB transmitter produces very short time domain pulses that are able to propagate through the space without the need of carrier frequency (carrier-free). Therefore, it is possible to design transmitter and receivers with fewer components.

Finally, it is worth to mention that thanks to its huge bandwidth, UWB systems can reach data-rates up to 1Gbps over very short range (less than 1m). The data rate can, however, be easily

traded-off for extension in range by simply using more or less concatenated pulses to define a bit (temporal diversity).

1.2.2 Applications

Thanks to the unique properties discussed above, UWB has lots of applications. Among its many applications includes:

- Radar imaging, ground penetrating radars (GPR), wall radar imaging, through-wall radar imaging
- Automotive radar for collision avoidance
- Short range wireless sensor networks (WSN) that combine positioning capabilities with low/medium data rate communications

Focusing a little more on that last point, we have the following applications:

- Security/Military: Locating authorized people in high-security areas and tracking the positions
- Inventory Control: Real-time tracking of shipments and valuable items in manufacturing plants, and locating medical equipments in hospitals.
- Smart Homes: Home security, control of home appliances, and locating inhabitants.

Accuracy requirements for these positioning scenarios vary depending on the specific application. However, for most applications, an accuracy of less than 30cm is required, which makes UWB a unique candidate in those scenarios.

1.3 Positioning Techniques

In order to estimate the position of a node ("Target" node) in a wireless network, signals are exchanged between the target node and a number of reference nodes ("Anchor" nodes) whose positions is known. The position of a target node can be estimated by the target node itself (self-positioning), or it can be estimated by a central unit that gathers position information from the reference nodes (remote-positioning), in this work we will only focus on the last one.

In general, the positioning problem is divided into two sub problems, in the first stage certain parameters are estimated from the signal and then they are used to estimate the target node position (two-step positioning). However, these two-stage methods are sub-optimal because in the first stage the signal parameters are estimated by ignoring the fact that all measurements should be consistent with a single target node. Therefore, the two-stage approach can be improved, especially in challenging scenarios, if the positioning problem is treat as a whole, that is, the target position is estimated directly from the signals received on each anchor node (Direct position estimation DPE). On the other hand, this improvement on the position estimation is at expense of complexity and computational load.

In this section, we will give an overview of the possible positioning techniques based on a two-step approach. The two-step approaches are mainly based on the estimation of the received signal strength (RSS), direction of arrival (DOA), time of arrival (TOA) or time difference of arrival (TDOA). It is also important to note that is possible to estimate multiple parameters per signal in order to improve positioning accuracy.

Finally, we will present several specific TOA estimation schemes for UWB systems.

1.3.1 Received Signal Strength (RSS)

In signal strength based positioning techniques, the distance between two nodes is calculated by measuring the energy of the received signal. Having a-priory knowledge of the distance dependency of the received signal power and of the transmitted one, the distance between the target node and the anchor node can be estimated.

The distance between two nodes provides a circle of uncertainty for the positioning of the target node. Therefore, a minimum of 3 distance measurements from 3 different nodes are necessary to determine the position. The target position will be given by the intersection of these 3 circles (trilateration, Fig. 3), however, due to inaccuracies the three circles will not intersect and therefore least squares solution is used as estimation.

The distance dependency comes from the path-loss which can be modeled as follows:

$$P(d) = P_0 - 10 \cdot n \cdot \log_{10}(d)$$

where *n* is the path-loss exponent, *P(d)* is the received power in dB at distance *d*, and P_0 is the transmitted power.

However, the received signal is affected by other factors such as shadowing effects, small-scale fading… As RSS measurements depend on the channel characteristics, RSS-based positioning algorithms are very sensitive to the estimation of channel parameters.

Just taking into account lognormal shadowing effects, the Cramer-Rao lower bound for the standard deviation of the unbiased estimated distance is:

$$\sigma_{\hat{d}} \geq \frac{(\ln 10) \cdot \sigma_{sh} \cdot d}{10 \cdot n}$$

Where *d* is the distance between the two nodes, *n* is the path-loss exponent and σ_{sh} is the shadowing standard deviation. As we can see in the expression above the accuracy of the distance estimation depends on the channel parameters and on the distance between the two nodes and not on the signal bandwidth. Therefore, the unique characteristic of UWB signals which is its large bandwidth is not exploited. That's why this method is barely applicable for UWB positioning.

Nevertheless, a general advantage of the RSS method is that no synchronization between the target node and the anchor node is required.

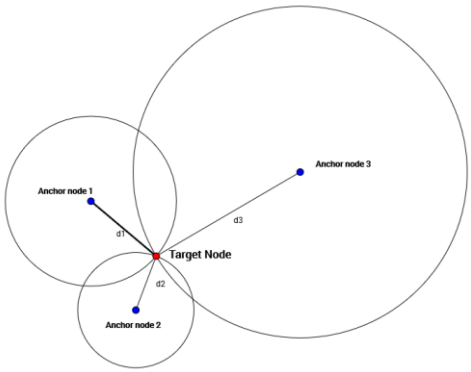

Fig. 3 Position estimation via trilateration

1.3.2 Direction of Arrival (DOA):

In Direction of arrival based positioning, the position of the target node is obtained by measuring the angles of the straight lines that connect the target node and at least 2 anchor nodes (triangulation), as shown in Fig.4.

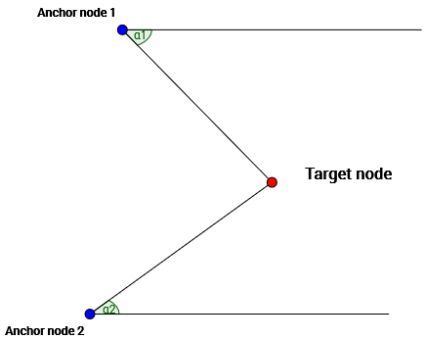

Fig.4 Position estimation via triangulation

Commonly, antenna arrays are employed to measure the DOA of a signal. The angle information is obtained by measuring the differences in arrival times of an incoming signal at different antenna elements. Depending on the geometry of antenna arrays the angle is related to the difference in arrival times on one way or another. For example, in a uniform linear array (Fig. 5)(ULA), the incoming signal arrives at consecutive array elements with $d \cdot \sin(\alpha)/c$ seconds difference, where d is the inter-element spacing, α is the DOA and c is the speed of light. Therefore, estimation of the time differences of arrivals provides angle information.

Under a single-path *additive white Gaussian noise (AWGN) channel*, the CRLB for the standard deviation of the unbiased estimated angle for a ULA with N elements is:

$$\sigma_{\hat{\alpha}} \geq \frac{\sqrt{3} \cdot c}{\sqrt{2} \cdot \pi \cdot \sqrt{SNR} \cdot \beta \cdot \sqrt{N \cdot (N^2 - 1)} \cdot d \cdot \cos(\alpha)}$$

Where α is the DOA, *SNR* is the signal-to-noise ratio and β is the effective bandwidth. It is noted that an increase in the SNR, effective bandwidth, inter-element spacing or the number of antenna elements improves the accuracy of DOA estimation. Therefore, unlike RSS methods, by using DOA methods we are taking advantage of the large bandwidth of UWB signal. However, this approach is not the most suitable for UWB systems as it requires antenna arrays which

increases the system complexity and the cost, annulling one of the main advantages of UWB systems which is low-cost transceivers.

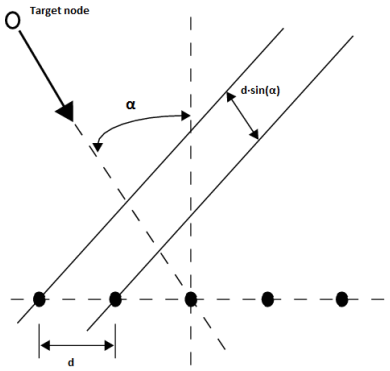

Fig. 5 ULA configuration and a signal arriving at the ULA with angle α.

1.3.2 Time-Based approach (TOA and TDOA):

TOA measurements provide information about the distances between two nodes by estimating the time of flight of a signal that travels from the target node to the anchor node. As in the RSS approach, by using the measurement of at least 3 distances the position can be trilaterated. This approach requires the nodes to be synchronized; nodes must either have a common clock, or exchange timing information by certain protocols such as two-way ranging protocol. This last protocol consists of measuring the round trip time (RTT) which is the length of time it takes for a signal to be sent plus the length of time it takes for an acknowledgment of that signal to be received,

$$RTT = 2 \cdot TOF + Tack$$

Where TOF is the time of flight that provides distance information and Tack is the time it takes the target node to process the received signal and start to transmit back.

When there is no synchronization between the target node and the anchor nodes, but there is synchronization among the anchors nodes, then Time Difference of Arrival (TDOA) techniques can be employed. In this case, the TDOA of two signals traveling between the target and two references nodes is estimated, which determines a hyperbola, with foci at the two reference nodes. Then, the position can be calculated as the intersection of at least two hyperboles, for which at least 3 anchor nodes are required.

Under a single-path *additive white Gaussian noise (AWGN) channel*, the CRLB for the standard deviation of the unbiased estimated time of arrival is:

$$\sigma_{\hat{\tau}} \geq \frac{1}{2 \cdot \sqrt{2} \cdot \pi \cdot \sqrt{SNR} \cdot \beta}$$

Where τ represents an unbiased TOA estimate, *SNR* is the signal-to-noise ratio, and β is the effective bandwidth. As we can see in the expression above the accuracy of the TOA estimation can be improved by increasing the SNR or the effective bandwidth. Therefore, large bandwidths of UWB signals can provide very precise TOA measurements. Moreover, they are less complex

and costly than DOA based approach. That's why, this technique has attracted the interest of the scientific community and the first commercially available UWB positioning systems are based on this approach.

The CRLB given above states that extremely accurate TOA estimation is possible in a single-path, line-of-sight (LOS) AWGN channel. However, real indoor environments are far more complex as multipath propagation and nonline-of-sight (NLOS) propagation can make accurate positioning very challenging. Fortunately, thanks to the high time resolution of the UWB signal, multipath components (MPC) are usually resolvable. Yet, it is still a factor to take into account.

Besides that, high time resolution of UWB signals makes it impractical to sample received signals at the Nyquist rate, which is typically on the order of a few GHz. Therefore, TOA estimation methods that can work at sub-Nyquist sampling rate are desirable for low power implementations.

1.3.3 TOA Estimation algorithms:

In this section, we will give a brief overview of the proposed TOA algorithm for UWB systems.

1.3.3.1 Matched – Filter

TOA estimation can be accomplished by the classical correlation estimator (or, equivalently, using a matched filter), where the TOA can be obtained by correlating the received signal with a template signal and choosing the time shift of the template signal that produces a maximum. The template signal should be the transmitted signal convolved with the channel impulse response; therefore, all the parameters regarding the channel response (multipath delays and attenuations) should be estimated. Since there are too many parameters to estimate, the conventional approach uses the transmitted signal (assuming *undistorted received pulses*) as a template, which makes it suboptimal. However, thanks to high time resolution of UWB signals, the multipath components do not overlap and then TOA can be accurately estimated by selecting the first peak above a certain threshold. The reason for selecting the first peak that surpasses a threshold and not the maximum absolute peak is because in indoor channels the first path may not be the strongest one.

However this approach has strong practical limitations as it requires sampling the output matched filter at the Nyquist rate. In this line, there are several proposes [7] to achieve a reliable TOA estimation sampling the output matched filter at symbol-rate or frame-rate, which is far lower than the Nyquist sampling rate.

When symbol-rate samples are employed, the TOA estimation can take a very long time. That is because the receiver needs to receive many symbols to accurately estimate the TOA. To address this problem, there are several proposes that consists of a two-step TOA estimation algorithm with an initial coarse estimation followed by a higher resolution stage.

1.3.3.2. Energy detector (non-coherent receiver)

This approach integrates the output of a *square-law* device over intervals comparables to the pulse width and then the TOA estimation is given by the first interval where the energy overcomes a suitable threshold [5]. The ranging accuracy of these schemes depends on the duration of the integration window which shall be selected to satisfy a good trade-off between accuracy and low sampling constraints (the sampling rate is given by the length of the integration window).

1.3.3.3. Maximum-Likelihood and Generalized Maximum-Likelihood

The exact maximum likelihood (ML) solution for the TOA estimation in UWB systems is known, however, it has strong practical limitations due to the requirements of very high sampling rates and complexity. To address this problem, there are several approaches that try to reduce the complexity [4]. However, there still exist practical limitations for their use in positioning applications.

Another approach is based on the Generalized Maximum Likelihood (GML) criterion to detect the TOA of the first path [8]. This method relies on the assumption that the number of multipath components is finite and known, and all the multipath coefficients and their arrival times are jointly estimated. In a typical indoor environment, the multipath is dense, the number of paths is large and unknown, and therefore, the GML is required to estimate too many parameters which include all the multipath arrival instants, amplitudes and phases. Thus, in dense multipath, the GML is not practical.

1.3.3.4 Frequency domain approach

TOA estimation has also been addressed applying frequency domain processing; these techniques are called “frequency-domain super-resolution TOA estimation”. By working on the frequency domain, time delay estimation becomes a frequency estimation problem and we can therefore apply spectral estimation techniques. In this context, high resolution spectral techniques such as Multiple Signal Classification (MUSIC) or root-MUSIC can be used as TOA estimators [6]. These methods are based on the separation of the signal and the noise subspaces. This characterization is associated with high computational load as it requires eigenvalue decomposition and besides that is not always reliable.

Another approach based on frequency domain processing, consists on using the periodogram spectral estimator. Thanks to the large signal bandwidth, periodogram spectral estimator can achieve high resolution TOA estimation at significantly lower complexity. Moreover, sampling requirements of frequency domain estimation methods can be significantly reduced when applying a channelization approach to the receiver architecture. We will discuss later about this particular approach as it is the basis upon this work is based.

1.3.3.5. Channel Impulse Response estimation algorithms

Algorithms to estimate the channel impulse response can also be used to estimate the TOA as the TOA is the first component of the channel impulse response. A classical approach to estimate the CIR is to deconvolve the received signal by dividing the spectrum of the received signal by the spectrum of the template and then taking the inverse Fourier transform. Better results can be obtained by using more sophisticated approaches such as the CLEAN algorithm which is a time domain deconvolution technique [15].

1.4 Compressive Sensing:

Although UWB systems are excellent candidates for positioning applications, its extremely large bandwidth requires a very high sampling rate which may be costly or even impractical. To overcome this constraint, compressive sensing (CS) [9] arises as a potential solution. Compressive sensing is a novel sensing technique that allows compressing signals with sparse or compressible representation while they are sampled, thus, it allows to sample a signal with a far lower rate than the Nyquist sampling limit.

CS relies on two principles: sparsity and incoherence:

Sparsity expresses the idea that the information conveyed in a signal may be much smaller than suggested by its bandwidth, or that a discrete-time signal depends on number of degrees of freedom which is comparably much smaller than its finite length.

Consider a real-valued, finite length, discrete time signal $x \in \mathbb{R}^M$ which can be expressed in orthonormal basis defined by the matrix $\underline{\underline{\Psi}} = [\underline{\psi_1}, \dots \underline{\psi_M}]$ as follows:

$$\underline{x} = \underline{\underline{\Psi}} \cdot \underline{\theta}$$

Then, sparsity refers that the vector $\underline{\theta}$ has few components different from 0. Therefore, if we want to represent the vector $\underline{x}$ we just need to know the K components different from 0 of $\underline{\theta}$ and the basis $\underline{\underline{\Psi}}$ which may be far less than the whole sequence $\underline{x}$.

Incoherence expresses the idea that signals having a sparse representation in the basis $\underline{\underline{\Psi}}$ must be spread out in the domain in which they are acquired. This is quite reasonable because if we sub-sample in the domain in which the signal is sparse it is very likely that we miss the non-zero coefficients of the signal, we must sub-sample in the domain in which the signal is spread out so as to capture the maximum information. To better illustrate this concept let's consider the classical discrete linear measurements model

$$\underline{y} = \underline{\underline{\phi}} \cdot \underline{x} = \underline{\underline{\phi}} \cdot \underline{\underline{\Psi}} \cdot \underline{\theta}$$

Where, $\underline{y}$ is the measured vector and $\underline{\underline{\phi}}$ is the sensing matrix, the typical sensing scheme would be $\underline{\underline{\phi}}$ equal to the identity. However, in CS we are concerned about sub-sampling therefore $\underline{\underline{\phi}}$ is rectangular matrix with fewer rows than columns, which means that the dimension of $\underline{y} \in \mathbb{R}^N$ is lower than $\underline{x}$. Then we want to recover $\underline{\theta}$ from the measurements $\underline{y}$. That is and ill-posed

problem with infinite solutions, however, we can use the constraint that $\underline{\theta}$ must be sparse to solve the problem. The optimization problem is the following:

$$\min\left\|\underline{\theta}\right\|_{l_0} \quad s.t\ \underline{y} = \underline{\underline{\phi}} \cdot \underline{\underline{\Psi}} \cdot \underline{\theta}$$

Where l_0 norm refers to the non-zero entries of the vector $\underline{\theta}$. Unfortunately, that is an NP-complete problem. So, instead of using the l_0 norm we can use the l_1 norm as it tends to sparsify the solution:

$$\min\left\|\underline{\theta}\right\|_{l_1} \quad s.t\ \underline{y} = \underline{\underline{\phi}} \cdot \underline{\underline{\Psi}} \cdot \underline{\theta} \qquad (1)$$

However, not all combinations of matrices $\underline{\underline{\phi}}$, $\underline{\underline{\Psi}}$ are suitable to recover the sparse vector $\underline{\theta}$. Regarding this topic, there is an important theorem that states that if the matrix $\underline{\underline{\phi}} \cdot \underline{\underline{\Psi}}$ holds the Restricted Isometry Property (RIP), the optimization problem in (1) provides an accurate reconstruction of $\underline{\theta}$.

Definiton For each integer S = 1,2…, define the isometry constant δ_S of a matrix A as the smallest number such that

$$(1-\delta_S)\cdot\|x\|^2{}_{l_2} \leq \|A\cdot x\|_{l_2}^2 \leq (1+\delta_S)\cdot\|x\|_{l_2}^2$$

Then, we will say that a matrix A obeys the RIP of order S if δ_S is not too close to one.

The natural question is: how can one design a matrix $\underline{\underline{\phi}}$, given the basis $\underline{\underline{\Psi}}$, so that $\underline{\underline{\phi}}$ holds for the RIP . Again, this is a NP-complete problem. However, if we design the matrix $\underline{\underline{\phi}}$ by sampling i.i.d entries from the normal distribution with mean 0 and variance 1/N, it will surprisingly obey the RIP with high probability.

Although the Compressive sensing framework looks very promising there is a substantial gap to bring all these ideas into real systems.

5. Methodology / project development:

This project is carried out at the department of Signal Theory and Communications (TSC) and is based on the previous works [1], [2], [3]. In this chapter we will review the ideas presented in these articles and we will present the developed ideas during this project.

1.1 Signal model

As we have discussed before the most suitable scheme for generating UWB signals is impulse radio UWB (IR-UWB). Impulse radio refers to the generation of a series of very short duration pulses. These pulses will have very low energy because of the very low power levels permitted. Therefore, many pulses will typically be combined to carry the information for one bit (temporal diversity), by doing that we achieve a processing gain that may be used to combat noise and interference.

The main advantages of this scheme are that the signal does not require a carrier frequency as the pulse will propagate well through the radio channel, furthermore, thanks to use of very short pulses with a low duty cycle the multipath components (MPC) can be resolved.

Taking all that into account, the transmitted signal is expressed as,

$$s(t) = \sum_{k=-\infty}^{\infty} \sum_{i=0}^{N_f-1} a_i \cdot p(t - (k \cdot N_f + i)T_f - c_i T_c - b_k T_\delta) \qquad (1)$$

The chosen modulation is Pulse Position Modulation (PPM) with $\{b_k\}$ being the information symbols taking values {0, 1}. Therefore, the bit information is conveyed by the timings of the pulses. T_f is the repetition pulse period (or frame period), N_f is the number of frames per symbol and T_δ is the PPM modulation interval. p(t) is the pulse waveform being typically a Gaussian monocycle or one of its derivatives .

In order to reduce the interferences to other systems, it is desirable to make the spectrum of the signal to look like noise (spectrum randomization). One way to achieve that is by randomizing the position of the transmitted UWB pulses in time (Time Hoping UWB, TH-UWB). The position in time is determined by a pseudorandom (PR) code which both transmitter and receiver need to know. Another technique to make the spectrum more noise-like is inverting the polarities of transmitted pulses randomly (Fig. 6).

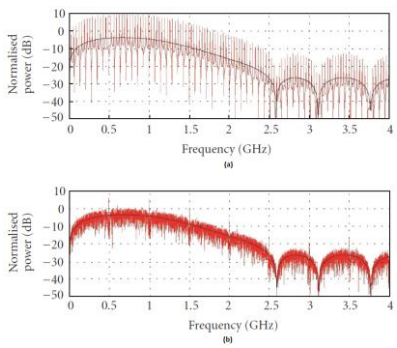

Fig. 6 (a) Spectrum without randomizing techniques (b) Spectrum with randomizing techniques [13]

Then, Tc is the chip period (the frame is divided into chips), {ci} is the pseudorandom time hopping sequence and a_i denotes the polarization sequence. Fig. 7 illustrates the time notation for the train of pulses.

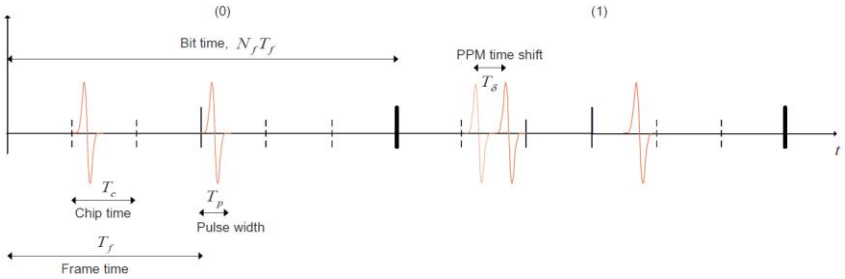

Fig. 7 Time notation for the train of pulses [1]

1.2 Channel model

The techniques developed in this work are tested under the IEEE 802.15.40 channels models, concretely the channel models CM-3[17]. A correct understanding of the peculiarities of UWB indoor radio propagation is fundamental to achieve good performance. In this section, the most important and peculiar features of the statistical characterization of UWB channels are studied.

Power delay profile and *small-scale fading* are those effects of the channel where the UWB propagation channel differs most significantly from narrowband channels. In a UWB channel, multipath components are distributed in clusters. The complex baseband impulse response of UWB channels is given by:

$$h(t) = \sum_{l=0}^{L} \sum_{k=0}^{K} \alpha_{k,l} \exp\left(j \cdot \phi_{k,l}\right) \delta(t - T_l - \tau_{k,l})$$

Where αk,l is the tap weight of the kth component in the lth cluster, Tl is the delay of the lth cluster, τk,l is the delay of the kth MPC relative to the lth cluster arrival time Tl. The phases ϕk,l are uniformly distributed within [0, 2π].

The distribution of the cluster arrival time and the ray arrival times are given by Poisson processes. The power delay profile is exponential within each cluster, and also the mean energy of the clusters follows an exponential decay. (Fig. 8)

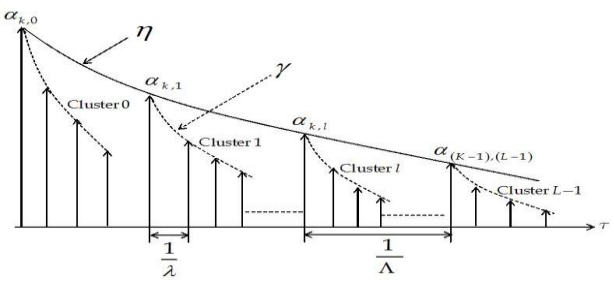

Fig. 8 Λ is the cluster arrival rate, λ is the ray arrival rate, αk,l is the tap weight, η is the cluster decay time constant and γ is the intra-cluster decay time constant

Small-scale fading refers to the variation in the amplitude of the channel coefficient $|\alpha_{k,l}|$, caused by the overlapping of unresolvable multipath components. In UWB channels is commonly modeled as a Nakagami distribution.

A UWB channel can often be modeled as a sparse channel in which the *delay spread* could be very large, but the number of significant paths is normally very small. Therefore, we can take advantage of that particular feature by using compressive sensing techniques.

1.3 Scenario

All the proposed techniques in this work are simulated on a squared room. However, when it comes to placing the anchor nodes an important question arises: "What is the optimal anchor node configuration?". To measure how well or bad is a particular anchor nodes configuration we must define some metrics. One possible metric is the CRLB of an unbiased estimator of the position (another possible metric would the DOP, which will be introduced later). Using this metric we are interested in finding the configuration that provides the minimum of the mean CRLB (by mean we refer to the CRLB averaged over the whole space).

Taking that into account the optimal configuration is depicted in the Fig. 9 [18]:

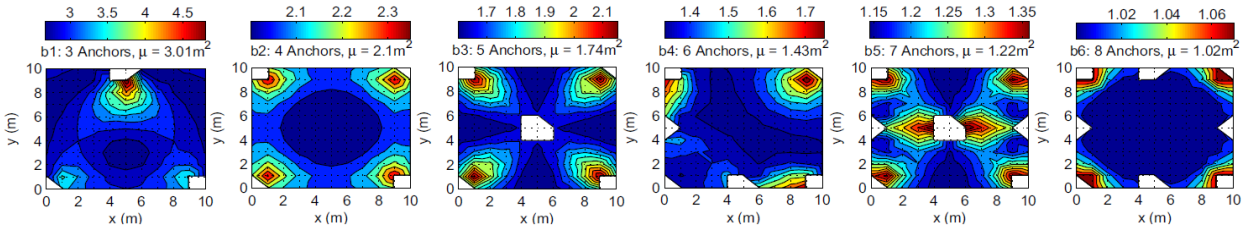

Fig. 9 Optimal anchor positions and corresponding CRLB for AWGN channels [18]

1.4 Frequency domain TOA estimation

In this section, we present the frequency domain TOA estimation technique which is the base for the rest of the project.

The transmitted signal introduced in the previous section is convolved with the channel model (the channel model given below is a general expression for the channel presented in the previous section):

$$h(t) = \sum_{m=0}^{M-1} h_m \cdot \delta(t - \tau_m) \qquad (2)$$

where τ_0 is the TOA to be estimated.

Therefore, the received signal can be expressed:

$$y(t) = \sum_{k=-\infty}^{\infty} \sum_{i=0}^{N_f-1} \sum_{m=0}^{M-1} h_m \cdot \tilde{p}\left(t - \Delta_{k,i} - \tau_m\right) + v(t) \qquad (3)$$

Where $\Delta_{k,l} = (k \cdot N_f + i)T_f - c_i \cdot T_c - b_k \cdot T_\delta$, $\tilde{p}(t)$ is the received pulse waveform which includes the receiver filter. The additive noise $v(t) \sim \mathcal{N}(0, N_0)$ is modeled as Gaussian circularly symmetric. Given the low duty cycle of UWB signals we can assume that the received signal is free of intersymbol interference (ISI).

Transforming the signal to the frequency domain, the signal associated to the ith transmitted pulse corresponding to the kth symbols is expressed as,

$$Y_{k,i}(\omega) = \sum_{m=0}^{M-1} h_m \cdot S_{k,i}(\omega) \cdot e^{-j\omega\tau_m} + V_{k,i}(\omega) \quad (X) \qquad (4)$$

with

$$S_{k,i}(\omega) = \tilde{P}(\omega)\, e^{-j\omega\left((k\cdot N_f+i)T_f+c_iT_c+b_kT\_\delta\right)}$$

where $\tilde{P}(\omega)$ is the Fourier transform of the pulse waveform $\tilde{p}(t)$ and $V_{k,i}(\omega)$ the noise in the frequency domain associated to the i-th frame interval corresponding to the k-th symbol. Sampling (4) at $\omega_n = \omega_0 \cdot n$ for n = 0,1, . . ., N and $\omega_0 = 2\pi/N$, and rearranging into a matrix notation the received signal is given by,

$$\underline{Y_{k,i}} = \underline{\underline{S_{k,i}}} \cdot \underline{\underline{E}} \cdot \underline{h} + \underline{V_{k,i}} \qquad (5)$$

where $\underline{Y_{k,i}} \in \mathbb{C}^{Nx1}$ is a vector containing the frequency samples of the signal, $\underline{\underline{S_{k,i}}} \in \mathbb{C}^{NxN}$ is a diagonal matrix which components are the frequency samples $S_{k,i}(\omega_n)$ and the matrix $\underline{\underline{E}} \in \mathbb{C}^{NxM}$ contains the delay-signature vectors associated to each arriving delayed signal (paths), $\underline{\underline{E}} = [\underline{e_{\tau_0}} \ \dots \ \underline{e_{\tau_m}} \ \dots \ \underline{e_{\tau_{M-1}}}]$ with column vectors being,

$$\underline{e_{\tau_m}} = \left[1 \ e^{-j\omega_o\tau_m} \ \dots e^{-j\omega_0(N-1)\tau_m}\right]^T$$

Fading coefficients are arranged in the vector $\underline{h} = [h_0 \ \dots \ h_{M-1}]^T \in \mathbb{C}^{Mx1}$ and the noise samples in vector $V_{k,i} \in \mathbb{C}^{Nx1}$.

As we are just interested in the first path we can rewrite (5) as,

$$\underline{Y_{k,i}} = \underline{\underline{S_{k,i}}} \cdot \underline{e_{\tau_0}} \cdot h_0 + \underline{\widetilde{V_{k,i}}} \qquad (6)$$

The estimation of the TOA becomes then a spectrum estimation problem. The motivation to consider a frequency domain approach is two-fold. On the one hand, frequency domain approaches allows for low complexity receiver architectures. This architecture is based on a bank of analog filters, which allow for sub-Nyquist sampling rate (Fig. 10). The filters are designed such that they form an orthogonal basis of the discrete time signal space which allows for an analog frequency-domain sampling of the received signal. The number of filters is a design parameter, which determines the dimensions of the receiver, and is directly related to the sampling rate and the acquisition time of the AD converts at which the receiver operates. On the second hand, frequency domain approaches have proven to provide high resolution for the estimation of the TOA.

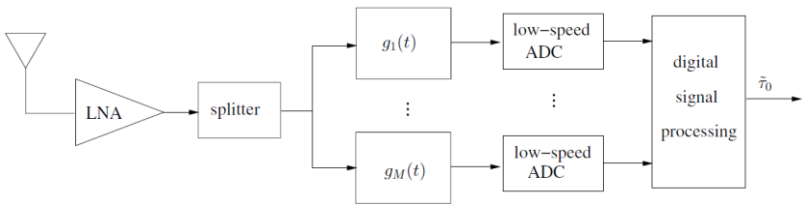

Fig. 10 Receiver block diagram [19]

Finally, we just have to decide which spectral estimator use. One option could be the minimum variance (MV) spectral estimator; however, given the inherent high time resolution of the UWB signal we can use less complex solutions such as the periodogram which does not require matrix inversion.

The periodogram in this particular case is an estimator of the power delay profile and can be obtained with the following expression.

$$P(\tau) = \underline{e_\tau}^H \cdot \underline{\underline{R}} \cdot \underline{e_\tau} \qquad (7)$$

Where $\underline{\underline{R}} \in \mathbb{C}^{NxN}$ is the correlation matrix which is computed by averaging over the N_f received frames. If more than one symbol is available for the TOA estimation, the correlation matrix is further averaged over the symbols,

$$\underline{\underline{R}} = \frac{1}{N_s \cdot N_f} \sum_{k=0}^{N_s-1} \underline{\underline{Y_k}} \cdot \underline{\underline{Y_k}}^H \qquad (8)$$

Where Ns is the number of symbols and $\underline{\underline{Y_k}} \in \mathbb{C}^{NxN_f}$ is a matrix whose columns are the vectors $\underline{\underline{Y_k}} = [\underline{Y_{k,0}} \ \dots \ \underline{Y_{k,i}} \ \dots \ \underline{Y_{k,N_f-1}}]$.

Then, the estimated TOA τ_0 is the first peak in the periodogram P(τ) that exceeds a certain threshold, the selection of the threshold is always a critical factor. Most of the proposals for the estimation of the threshold require some heuristic adjustment.

1.4 DPE

As we have discussed in the previous chapter, the position estimation performance can be potentially improved if one treats the positioning problem as a whole. Instead of estimating certain parameters of the received signal at each anchor node and then finding the position by trilateration, one can achieve better results if the position is estimated directly from the combination of the signals received at each anchor node.

In this section, we present a Direct Position Estimation (DPE) technique based on the periodogram presented before. By using this approach we not only achieve better performance but also overcome the problem of threshold setting required in the TOA estimation problem. However, this improvement is at expenses of higher computational load and the requirement of transmitting the whole received signal to a central processing node.

The DPE problem can be formulated as follows:

Lets define the observation frequency sample vector as the concatenation of signals received from all anchors, $\underline{Y_{k,i}} = \left[\underline{Y_{k,i}}^{(1)}, \dots, \underline{Y_{k,i}}^{(l)}, \dots, \underline{Y_{k,i}}^{(N_A)}\right]^T \in \mathbb{C}^{N \cdot N_A \ x \ 1}$, where N_A is the number of anchors nodes. The system model can then be written as (symbol and pulses indexes are dropped),

$$\underline{Y} = \underline{\overline{S}} \cdot \underline{e_p} + \underline{\tilde{V}} \quad (9)$$

where, $\underline{\overline{S}} = diag\left(h_{0,1} \cdot \underline{S}, \dots, h_{o,N_A} \cdot \underline{S}\right) \in \mathbb{C}^{N \cdot N_A \, x \, N \cdot N_A}$, $\underline{e_p} = \left[\underline{e_{f_1(p)}}, \dots, \underline{e_{f_{N_A}(p)}}\right] \in \mathbb{C}^{N \cdot N_A \, x \, 1}$ and $\underline{\tilde{V}} = \left[\underline{\tilde{V}}^{(1)}, \dots, \underline{\tilde{V}}^{(N_A)}\right]^T$. The delay-signature vectors $\underline{e_{f_1(p)}}$ are the same as in the TOA estimation but expressed in terms of the target spatial coordinates, then $f_l(p) = \frac{\|p - p_l\|}{c}$, where p_l are the coordinates of the lth anchor in the space and c is the speed of light.

Finally, the estimated position is the one that maximizes the following cost function (joint periodogram),

$$\hat{p} = argmax_{p \in \mathbb{R}^2} \, \underline{e_p^H} \cdot \underline{\underline{R}} \cdot \underline{e_p} \quad (10)$$

Where, $\underline{\underline{R}} = \frac{1}{N_s \cdot N_f} \sum_{k=0}^{N_s - 1} \sum_{i=0}^{N_f - 1} \underline{Y_{k,i}}$

The cost function is maximized in a greedy manner by grid search over the two dimensional space (Fig. 11).

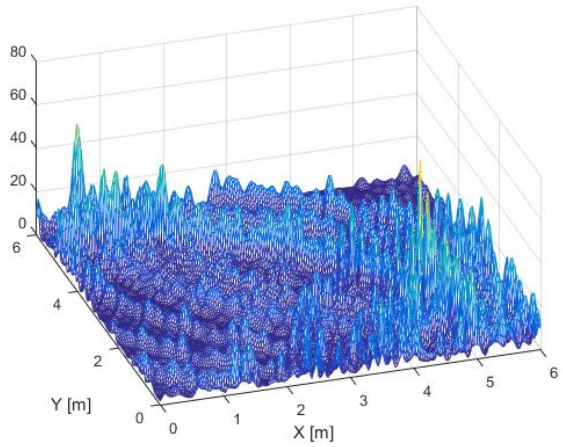

Fig. 11 Joint Peridogram for 4 anchors

1.5 DPE-DOP

Once we have presented the basis upon which this work is build, we can introduce the proposed improvements for these particular techniques.

The main sources of errors in the DPE technique presented before come from the fact that UWB channels (in that case, CM3) are very harsh environments with dense multipath components. Furthermore, these channels are not classical LOS scenarios where the LOS is present with stronger amplitude than other multipath components. In fact, there are channel realizations where delayed multipaths are considerably larger than the LOS (Fig. 12).

By using this technique, we expect the true target position to be the one that gives a maximum in the cost function, that's reasonable because the true target position will be the one gathering energy from all the anchor nodes. However, given the fact that multipath components may be quite larger than the first path it may happen that the intersection of two high energy multipath components gives a higher value than the true position.

The first idea to address the problem is to select the region with higher energy instead of the absolute maximum. The neighborhood of the true position is expected to have more energy than other regions because it will surely gather energy coming from all the anchor nodes. Just by taking the maximum it could happen that the energy belonging to each anchor node did not converge into a single point and therefore it was more sensible to multipath effect.

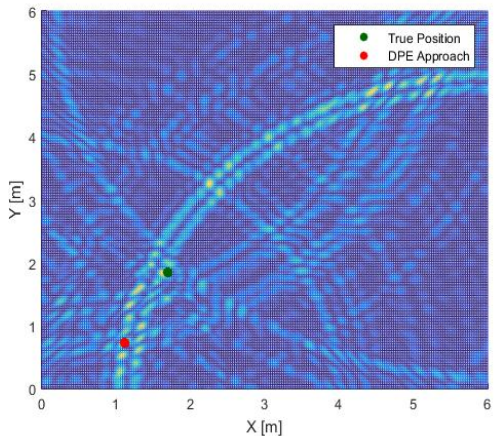

Fig. 12 DPE approach with 4 anchor nodes, error caused by strong multipath

Then, we must define this region or neighborhood around every single point in the 2D space. A logical approach would be to take all the area of uncertainty if that particular point were the real solution. To better explain that we introduce the concept of Dilution of Precision (DOP). DOP is an indicator of 2-dimensional positioning accuracy as a consequence of relative position of anchor nodes with respect to the target node, a cumbersome way to express it would be:

$$DOP = \frac{Positioning\ Error}{Ranging\ Error}$$

Fig. 13 explain a simple interpretation for this,

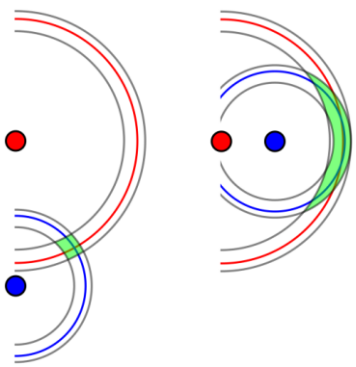

Fig. 13 a) Low DOP b) High DOP

In Fig. 13 a) and b) there is the same ranging variance, however, the region of uncertainty (the green area) is much smaller in a).

Therefore, for a given anchor nodes configuration, expected variance in the measurements and point in the space we can calculate this area (Fig. 14). Once we have found the area, we just have to integrate the cost function under that area, repeat that for every single point of the grid search and pick the maximum (Fig. 16). Basically, by doing that we are low pass filtering the 2D cost function with space-variant filter.

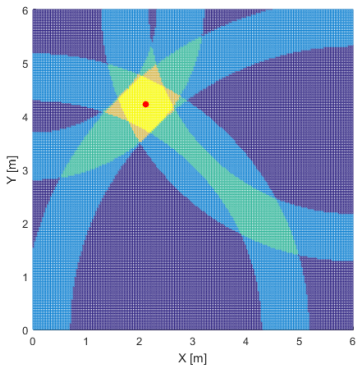

Fig. 14 Uncertainty area for 4 anchor nodes

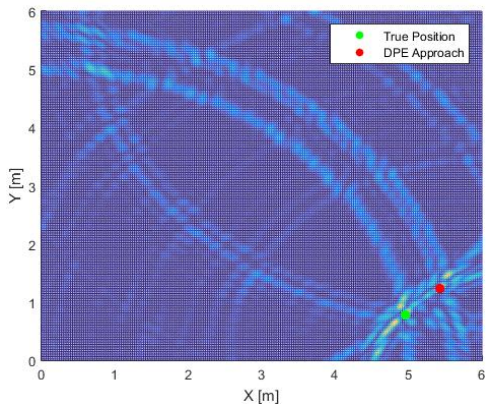

Fig. 15 DPE approach fails to position the target node due to strong multipath

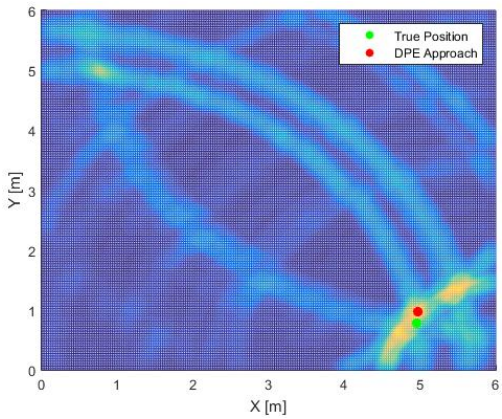

Fig. 16 DPE-DOP solves the strong multipath problem

1.6 MultiTOA

In the previous approach we tried to mitigate the fact that the multipath delays were much stronger than the LOS by integrating the two dimensional cost function in certain areas. The areas around the true position are supposed to gather much energy because there is contribution of all the anchor nodes, whereas, the areas around the crossing of strong multipath will just contain noise. However, the LOS may be so attenuated with respect to other multipath components that, in many cases, it is not enough to overcome the problem.

In the next solution we change completely the way to face the problem. We forget about combining the signals received in all the anchors nodes, and we go back to the estimation of the TOA. As the periodogram estimated in each anchor are not functions to be maximized but instead we are interested in the first peak, it is not optimal to combine the signals summing them because then we lost the idea that first peaks are more important than strong peaks. Therefore,

as there is no straightforward way to combine the periodograms into a "joint periodogram" we decided to go back to the TOA estimation and design new techniques.

If we recall, the estimated TOA is the first peak in the periodogram that exceeds a certain threshold, and the selection of that threshold is always a critical factor that may drop the performance drastically if it is not chosen properly. Then, the proposed solution is the following: instead of setting a threshold and keeping the first peak above it, we select all the prominent peaks (Fig. 17)(as the periodogram is noisy, we set a really low threshold to avoid having a huge number of peaks) and then we use all potential TOA to find the position. All the potential TOA are gathered in the central processing unit and the combination of TOAs that minimize the trilateration cost function are the ones selected, and therefore, the estimated position will be the solution of that particular trilateration (Fig. 18). In other words, we will select the position that minimizes the following cost function:

$$J\left(\underline{p}, \underline{k}\right) = \sum_{l=1}^{N_A} \left(\tau_l[k_l] \cdot c - \left\|\underline{p} - \underline{p_l}\right\|\right)^2 \qquad (11)$$

where $\underline{p} \in \mathbb{R}^2$ is the estimated position, $\underline{p_l} \in \mathbb{R}^2$ is the position of the lth anchor node, c is the speed of light and $\tau_l[k_l]$ $k_l \in \{1, \dots, m_l\}$ are all the potential TOAs detected in the lth anchor node.

By doing that we are mitigating the strong multipath components because all possible delays are given the same weight. We are not taking into account how strong a delay is because that information is not very reliable, instead, we are deciding according to how consistent the delays are.

Moreover, whereas the DPE approach requires transmitting the whole signal to the central processing node, it just requires transmitting the potential TOAs which is far less data.

Up to this point, Compressive Sensing was applied over the 2D space and it was based on the spatial sparseness of the problem (the number of unknown targets is very small). However, now we can take advantage of the sparsity of the UWB channels and further exploit their structure. As MPC components are arranged in clusters we can use that information to design more efficient sensing techniques. For more details, we refer the reader to the thesis developed by Ricard Garcia.

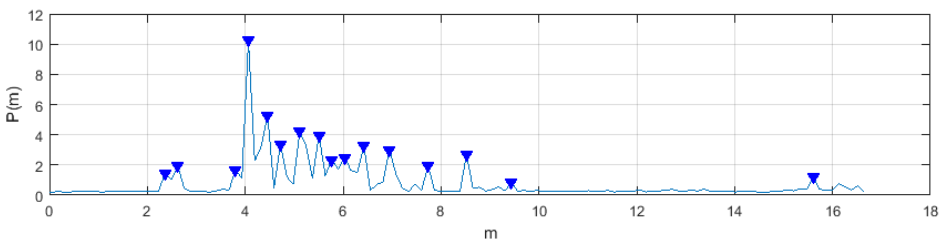

Fig. 17 Periodogram and the selected peaks

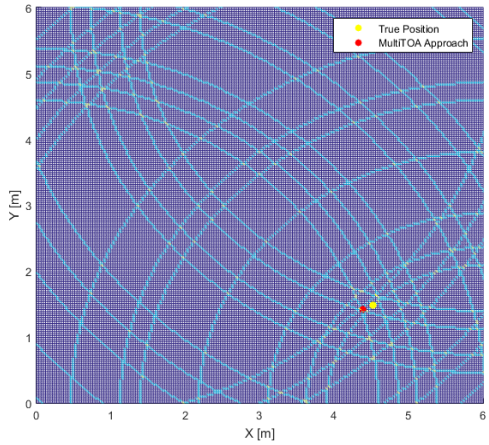

Fig. 18 Detected peaks represented in the 2D plane and the MultiTOA approach

1.6.1 Trilateration algorithm

Before tackling the problem of solving (11) we will discuss how to solve the trilateration problem. The trilateration problem can be seen as a ML estimator of the position given noisy measurements, whose solution is given by solving a Non Linear Least Squares problem, where the goal is to minimize the following cost function (if variances in the TOA estimation are not known we set them equal to 1):

$$\hat{\underline{p}} = argmin_{\underline{p}}\{\sum_{l=1}^{N_A} \frac{\left(\tau_l \cdot c \; - \left\|\underline{p} - \underline{p_l}\right\|\right)^2}{\sigma_{\tau_l}^2}\} \qquad (12)$$

One approach to solve this optimization problem is using linearization techniques, and then the problem becomes a Linear Least squares problem that can be solved using the pseudoinverse. However, the accuracy of this approach may be quite low and moreover we must take care about singular or poorly conditioned matrices.

Another approach could be using gradient descent algorithms such as Gauss-Newton or Levenberg-Marquardt. However, the cost function (12) may have many local minima and saddle-points which can make gradient descent algorithms to converge erroneously.

To overcome this shortcoming, we have decided to use the well-known Projection onto convex sets (POCS) algorithm [10] [11] which has shown to be robust to local minima while offering low complexity and good performance. In this case, the problem is formulated as a convex feasibility instead of non linear least squares.

Each term in the sum of (12) obtains its minimum on the circumference of disc:

$$D_l = \{\underline{p} \in \mathbb{R}^2 : \left\|\underline{p} - p_l\right\| \leq \tau_l \cdot c\}$$

An estimator of the target node position would be any point the intersection *D* of the convex sets D_l:

$$\hat{\underline{p}} \in D = \cap_{l=1}^{N_A} D_l$$

Due to noise in the measurements the intersection D might be empty, and then the estimated position will be:

$$\hat{\underline{p}} = argmin_{\underline{p}} \sum_{l=1}^{N_A} \left\| \underline{p} - \mathcal{P}_{D_l}(\underline{p}) \right\|$$

Where $\mathcal{P}_{D_l}(\underline{p})$ is the projection of the point p onto the convex set D_l, which in the case of a disc is:

$$\mathcal{P}_{D_l}\left(\underline{p}\right) = \begin{cases} \underline{p} & if \quad \left\| \underline{p} - p_l \right\| \leq \tau_l \cdot c \\ \underline{p_l} + \tau_l \cdot c \cdot \dfrac{\underline{p} - \underline{p_l}}{\left\| \underline{p} - \underline{p_l} \right\|} & otherwise \end{cases}$$

Then, what this algorithm does is project onto the different convex sets iteratively. The steps taken are the following:

1. Initialize $\underline{p}^0$ arbritarly
2. Iteratively:

$$\underline{p}^{k+1} = \underline{p}^k + \lambda_k \cdot \left[\mathcal{P}_{D_{k(k)}}\left(\underline{p}^k\right) - \underline{p}^k \right]$$

Where, $k(k) = k \ mod \ N_A$ (iterate cyclically onto the different convex sets) and λ_k are relaxation parameters. Normally, relaxation parameters are initially set to 1 and after a certain numbers of iterations (k_0) is decreased at a rate 1/(k- k_0).

This algorithm can be more easily understood if we take a look at the path that it follows to solve the trilateration problem (Fig. 19).

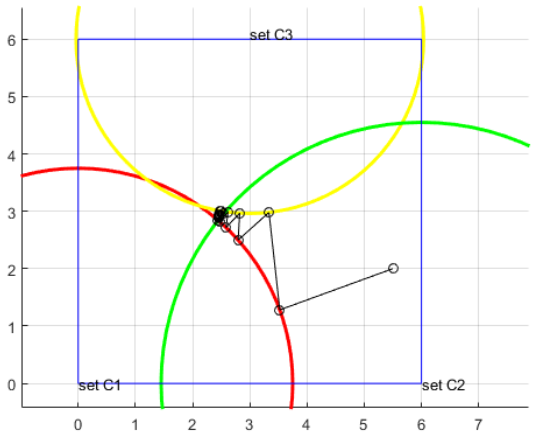

Fig. 19 Path for POCS solving the intersection of 3 discs

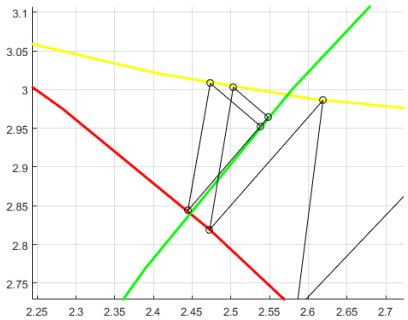

Fig. 21 λ set to 1

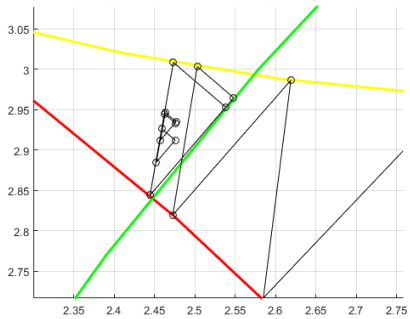

Fig. 20 Effect of decreasing λ

The unique drawback of this algorithm is that when the target node is located outside the convex hull of the anchor nodes it exhibits poor performance (Fig. 22). That's because the area of D becomes larger if the target node is located far from the convex hull (orange triangle in Fig. 22).

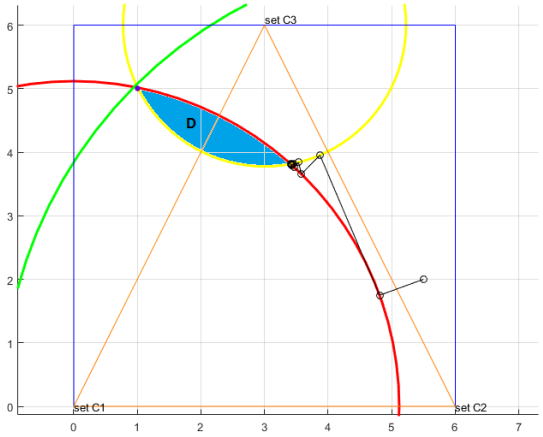

Fig. 22 POCS converging erroneously

In the case when the measurement noise (σ_{τ_l} in (12)) is small, we can improve the POCS algorithm by projecting onto a ring (POR) instead of a disc. The width is a parameter related to the noise in the measurements. However, as this noise is unknown we simply set the width to 0, projecting then into a circumference. By doing that, we overcome the problem present when the target node is outside the convex hull (Fig. 23).

Fig. 23 Projection onto rings finding the target node located outside the convex hull

1.6.2 MultiTOA cost function

When it comes to solving the cost function in (11) we must deal with a function that depends on discrete variables (the variable k). Address this discrete optimization problem by brute force, which is trying all the possible combinations, is not feasible, as the number of combinations grows exponentially with the number of anchor nodes ($\#combinations = \prod_{l=1}^{N_A} m_l \approx m^{N_A}$, assuming that all nodes provide the same number of peaks) . For instance, in a scenario of 5 anchor nodes and 16 peaks (as in the periodogram in Fig. 17) there are more than 1 million of combinations.

Grid Search:

One approach could be discretize the 2D space solution and solve the problem by exhaustive grid search. Then, for every point in the grid we should sum the distances to the closest delays of each anchor node (Fig. 25). An example of the resulted cost function can be seen in Fig. 24.

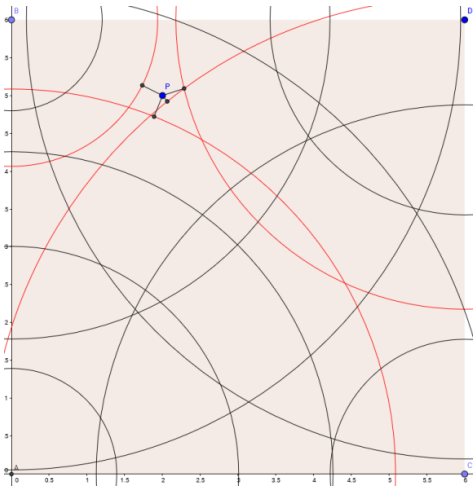

Fig. 25 Evaluation cost function at point P.

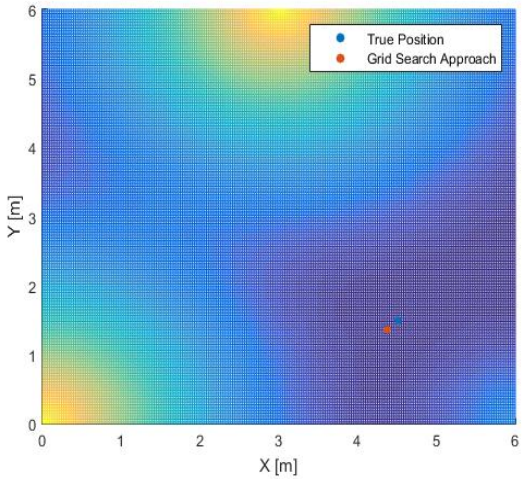

Fig. 24 Discretized cost function

This approach can be speed up by dividing the search in two-steps. First, the cost function is evaluated for a discrete grid of positions with relatively wide spacing. The set of *U* positions that attain lowest cost function values are used as initial estimates for a second search phase. In the second search phase, a fine search is conducted in the vicinity of each initial estimate to find a position that attains local minimal cost function.

Branch and Bound, Best First search:

A very different approach could be to solve the discrete optimization problem by using discrete optimization techniques. The chosen algorithm to solve the optimization problem is “Branch and Bound” which is based on the algorithm design paradigm of divide and conquer. A divide and conquer algorithm works by recursively breaking down a problem into two or more sub-problems which are easier to solve than the actual problem. Branch and Bound in particular is a tree-search based algorithm where each node of the tree is a subproblem, then after solving a sub-problem we can set a bound about how good the final solution (leaves of the tree) could potentially be if we kept descending in the tree through that node. If that bound is better than an already found solution we have to expand this node and explore its children, however, if that bound is not better than an already found solution we can prune that node, thus reducing the search space.

From this point onwards, to avoid confusions, we will refer the anchor nodes as beacons and the nodes of a tree as nodes.

In our particular problem, the elements of the tree would be:

- Nodes: A particular trilateration using fewer beacons than the available. The depth of the tree is equal to the number of beacons
- Lower Bound: The cost of that particular trilateration
- Children: The children of a given parent node are the trilaterations using the same parameters of the parent node but adding the TOA information of the new beacon (the number of children is equal to the number of potential TOAs estimated by the new beacon)
- Leaves: A possible solution of the problem, there are as many leafs as number of combinations ($\prod_{l=1}^{N_A} m_l \approx m^{N_A}$).

The way to explore the tree is a key factor to find the solution quickly. We have chosen the best-first search strategy which explores the tree by expanding the most promising node.

The steps of the algorithm are the following:

1. Create priority queue (queue that pops the elements with higher priority (0 means high priority while ∞ means low priority))
2. Select two arbitrary, beacons $\underline{p_1}$, $\underline{p_2}$ and compute all the 2 by 2 intersections of the circles defined by the TOAs measured on these beacons. The bound for those combinations that intersect will be 0 whereas the bound for those who do not intersect will $\frac{1}{2} \cdot dist(d_1, d_2)$, where dist is the distance between the two circles. Then, these nodes will be added to the queue setting the priority equal to bound. The information stored in each node of the tree (or item in the queue) is the beacons used, the potential TOA used for each beacon, the value of the bound and the estimated position if only these beacons were available.
3. Set $J = \infty$
4. While queue is not empty:
    i. Remove the most priority node of the queue, call it topNode.
    ii. If topNode.bound < J
    iii. Explore children of topNode and add them to the queue
    iv. if children are leaves and the computed bound is lower than J update J
    v. End if

To better understand the algorithm, in Fig. 26 we can see the tree generated for the case of 3 beacons with 2 measured TOAs per beacon (that is a discrete optimization problem with 3 binary variables).

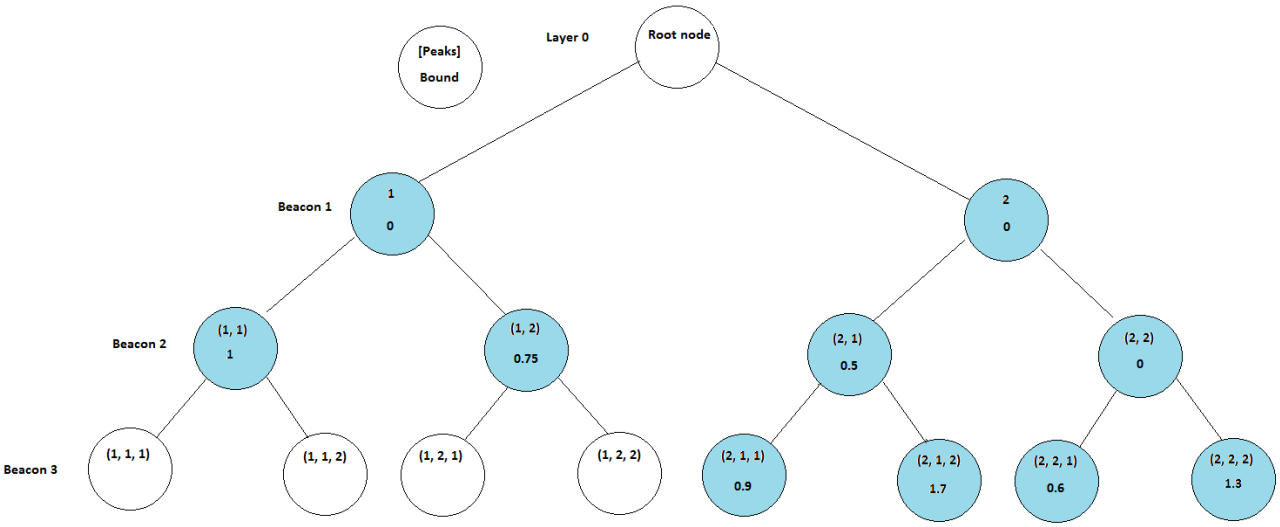

Fig. 26. Nodes (1,1) and (1,2) do not need to be expanded because the bound of their children will be at least 1 and 0.75 respectively, which is higher than the already found solution 0.6.

This algorithm can be further improved if we realize that when a node is expanded it is not necessary to compute the bound for all the children. That is because the most promising children will always be the one whose associated TOA (the circle defined by the TOA measurements) is closest to the position estimated in the parent node, then all the other children can be bounded by the same value. It is important to note that these children cannot be pruned because the forthcoming TOAs of the next beacons may give better final solutions using those children that gave worse bound. (Fig. 27)

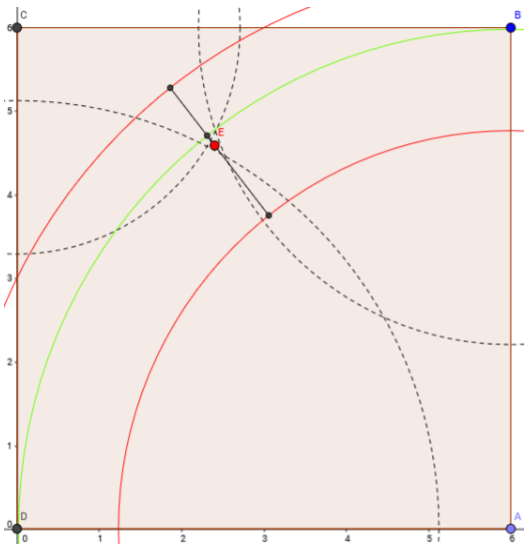

Fig. 27 As red circles are farther from the point E than the green circle we do not need to find the trilatetion for these combinations.

In Fig. 28 we can see the number of nodes visited for the proposed algorithm in a scenario with 5 beacons and the channel realizations in Fig. 28. In this case, brute force algorithm would require to compute 7·20·12·20·18 = 604800 trilaterations of 5 beacons whereas the proposed just requires to compute 36 trilaterations with 2 beacons, 106 with 3 beacons, 24 with 4 beacons and 3 with 5 beacons which is much less than the 604800.

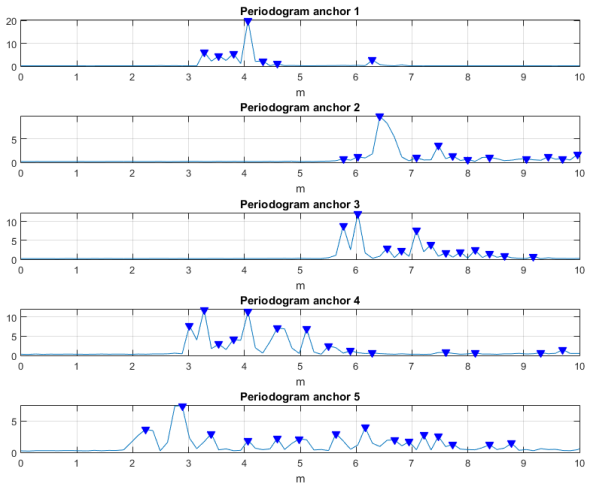

Fig. 28 Peaks detected in a scenario with 5 beacons

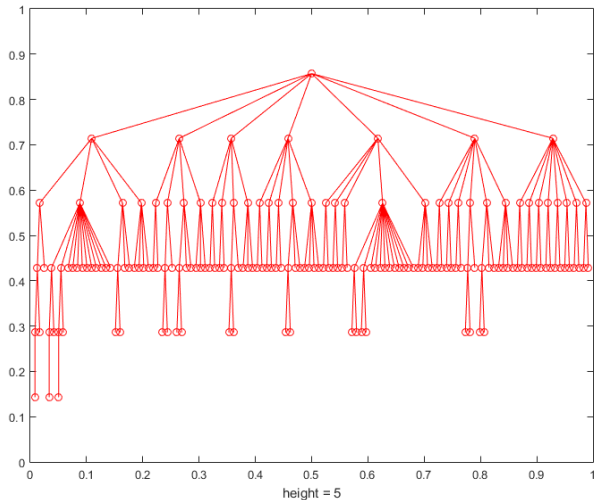

Fig. 29 Tree generated by the branch and bound algorithm

1.6 MultiTOA Weighted

In the previous section we presented the MultiTOA position algorithm. It was based on the idea that energy of paths detected on the periodagram is not reliable because the LOS could be highly attenuated. Therefore, we designed an algorithm merely based on the consistency of the delays calculated in each beacon, ignoring then, the energy of the peak and the relative position of that peak in the periodogram. The probability of error, that is selecting a combination of multipaths that do not represent the real position, is quite low because each beacon sees a different channel realization and therefore the position of the multipath is completely random. However in the case of using very few beacons it tends to happen quite often (Fig. 30).

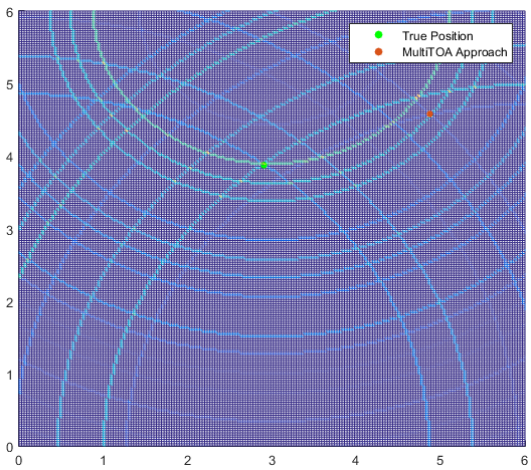

Fig. 30 MultiTOA fails to position the target node as there are multipath components that intersect more consistently

To overcome that problem we decided to incorporate information about energy and relative position in the periodogram into the cost function to be minimized. By inspecting one periodogram realization (Fig. 31) we realize that it is not necessary to collect all the prominent peaks. For example in the Fig. 31, the last peak to be the true TOA would mean that all the previous peaks were noise or pulse sidelobes of that peak and such thing is highly unlikely.

To attain this problem we decided to weight each peak by the probability of that peak being the true TOA. By weighting the peaks we improve the overall performance of the position estimation technique because the number of peaks gets reduced (last peaks will have probability 0 so we remove them) so it will be easier to minimize the cost function, and moreover we reduce the probability of choosing path that do not represent the position of the target.

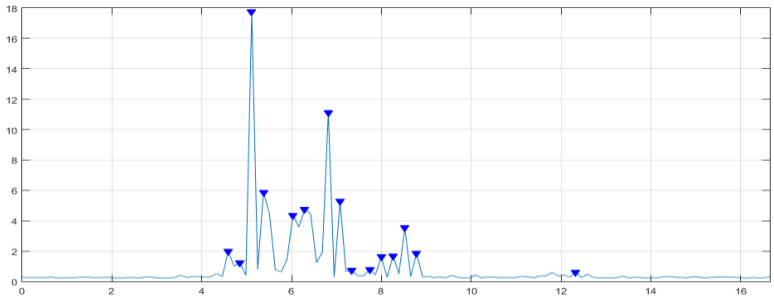

Fig. 31 It is clear that the third peak cannot be caused by noise or sidelobes. Therefore the later peaks should be rejected.

However, as it happened with threshold selection (in the pure TOA periodogram approach), finding these probabilities is not an easy task. Then, the weighting criterion is based on the distribution of the early peaks, which are the peaks that appear before the true TOA. A given peak will have larger weight as less probable it is to be a false peak, that is:

$$Weight_{pea\,k_i} = 1 - P_e = 1 - P(E_{ep} > E_{pea\,k_i})$$

Where, E_{ep} is the random variable that represents the energy of the early peaks and E_{peaki} is the Energy of a i*th* detected peak. However, these probabilities should be conditioned to the fact that previous peak was not the true TOA, then:

$$Weight_{pea\,k_i} = \prod_{k=1}^{i-1}\left(1 - Weight_{pea\,k_k}\right) \cdot \left(1 - P\left(E_{ep} > E_{pea\,k_i}\right)\right)$$

The energy of the early peaks depends on the noise level as well as the pulse sidelobes of the true TOA and later multipath components. Then, to find the analytical distribution of these peaks we should consider the distribution of the fading coefficients that follows a Nakagami distribution, the multipath arrival time that follows a Poisson distribution, the power delay profile that is and exponential decay and the noise that is Gaussian. Therefore, finding the analytical distribution is extremely complex as it depends on too many parameters. So, instead of finding the exact analytical distribution, we have estimated it by running a large number of simulations and then using a kernel density estimator, in this case a Gaussian kernel. The distribution of the early peaks and the true TOA is depicted in Fig.32.

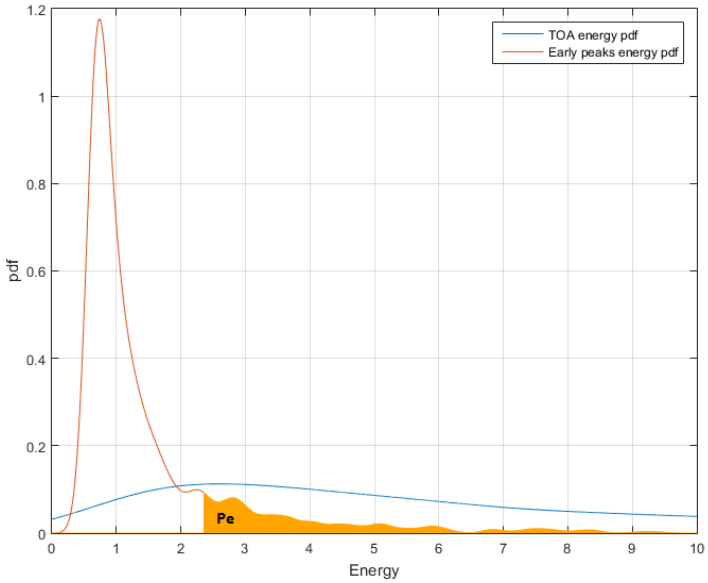

Fig. 32 Empirical pdfs

In order to consider these weights, we have to modify the cost function in (11):

$$J\left(\underline{p}, \underline{k}\right) = \sum_{l=1}^{N_A} \left(\tau_l[k_l] \cdot c - \left\|\underline{p} - \underline{p_l}\right\|\right)^2 + \lambda \left(-\sum_{l=1}^{N_A} Weight_l[k_l]\right)$$

where, $Weight_l[k_l]$ $k_l \in \{1, \dots, m_l\}$ is the weight of the k_l peak of the *lth* anchor node and the parameter λ is a trade-off between consistency of the delays and probability of the delays. If our measurements are not vey noise which means that the delays will be very consistent we will use a small lambda, if not, we should increase it.

It is important to note that the branch and bound algorithm should be adapted to this new cost function. Now, in order to prune a node we should consider the peaks in the children of that node to have weight equal to 1. That is, we can just prune a node if the bound computed in that node minus $\lambda \cdot (N_A\text{-depthNode})$ is higher than an already found solution.

6. Results

In this chapter, the three proposed position estimation techniques presented in the previous chapter (DPE-DOP, MultiTOA and MultiTOAWeighted) are assessed to evaluate their performance and find out if they provide any improvement with respect to the baseline estimators.

The algorithms have been analyzed by means of Monte-Carlo MATLAB-based simulations. For numerical evaluation we consider the channel models developed within the framework of the IEEE 802.15.4a [17]. In particular we evaluated the localization performance for the CM3 Office LOS which is the channel that presents more difficulties due to the strong LOS attenuation.

The positioning algorithm is evaluated in a 2D setting with the target randomly placed within a square room of 6x6 m^2. The anchor nodes have been placed according to Fig. 9. In all simulations we have considered 500 channel realizations.

In the following table there are summarized the parameters related to the IR-UWB signal model that remain constant throughout the simulations.

$\mathbf{T_p}$ (Pulse duration)	1 ns
$\mathbf{T_f}$ (Time of frame)	56 ns
$\mathbf{F_s}$ (Sampling frequency)	2 GHz
$\mathbf{N_f}$ (Number of frames)	128

Table. 1 Signal parameters

The performance of the algorithms will be measured according to the empirical cumulative density function (ecdf) of the error and root mean squared error (RMSE) defined as $RMSE = \sqrt{\frac{1}{N}(Err_1^2 + \ldots + Err_N^2)}$, where N are the number of channels simulated and Err_i is the error committed in the ith channel realization . These are good indicators of the accuracy and precision of the algorithms.

4.1 DPE-DOP

The next simulation has been performed using 4 anchor nodes. The room is divided into a 200x200 grid and hence the resolution is 6/200 = 3cm. We consider a SNR at each anchor node of 4dB.

	RMSE
DPE	1.19m
DPE DOP	1.09m

Table. 2 RMSE for the DPE-DOP approach

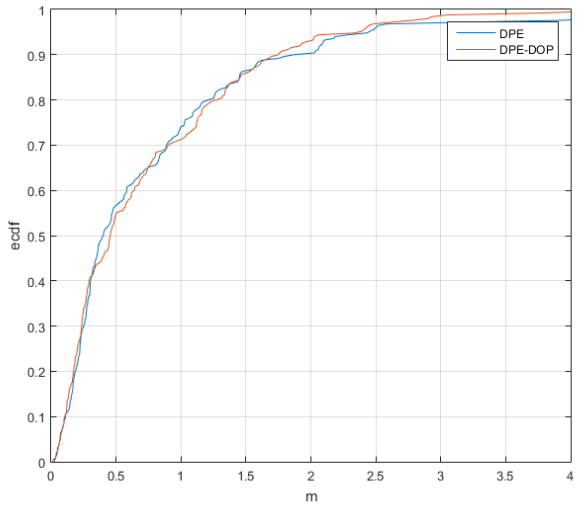

Fig. 33 Empirical cdf of the error for the DPE and DPE-DOP approach

We can see that the improvement of the DPE-DOP approach with respect to the baseline DOP is almost imperceptible.

4.2 MultiTOA

The following simulation has also been performed using 4 anchors node, with a SNR at each anchor node of 4dB. To solve the optimization problem we have used both the grid-search approach (again with 3cm resolution) and the Branch and Bound algorithm presented in the previous chapter.

	RMSE
DPE	1.19m
MultiTOA Grid	0.3m
MultiTOA B&B	0.27m

Table. 3 RMSE for the MultiTOA approach with 4 anchor nodes

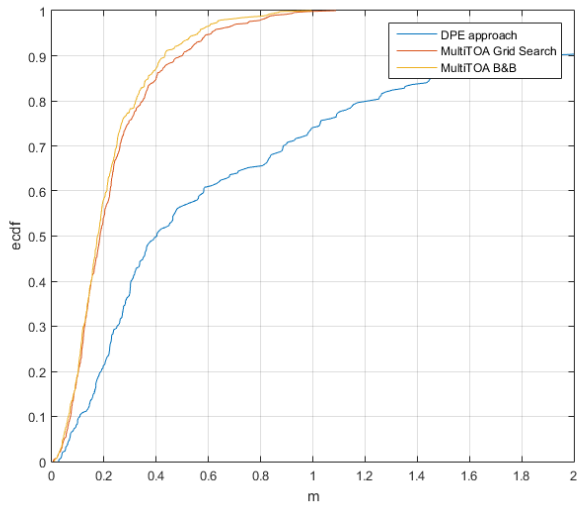

Fig. 34 Empirical cdf of the error for the DPE, MultiTOA B&B and GridSearch approach with 4 anchor nodes

By looking at the ecdf we can see that the proposed algorithm performs much better than the DPE approach. Therefore, we can conclude that the proposed algorithm does work and overcomes the strong LOS attenuation as well as the dense multipath present in indoor UWB channels.

We can also appreciate that the Branch and Bound solution is slightly better than the Grid Search, that may be because in the Grid Search the resolution is set to 3cm whereas in the Branch and Bound there is no resolution limit. It is also important to highly that the Branch and Bound approach is quite faster than the Grid Search approach.

We have also tested the MultiTOA algorithm in a scenario with just 3 anchor nodes and SNR equal to 4dB in each anchor node.

	RMSE
DPE	1.74m
MultiTOA Grid Search	1.23m
MultiTOA B&B	1.1m

Table. 4 RMSE for the MultiTOA approach with 3 anchor

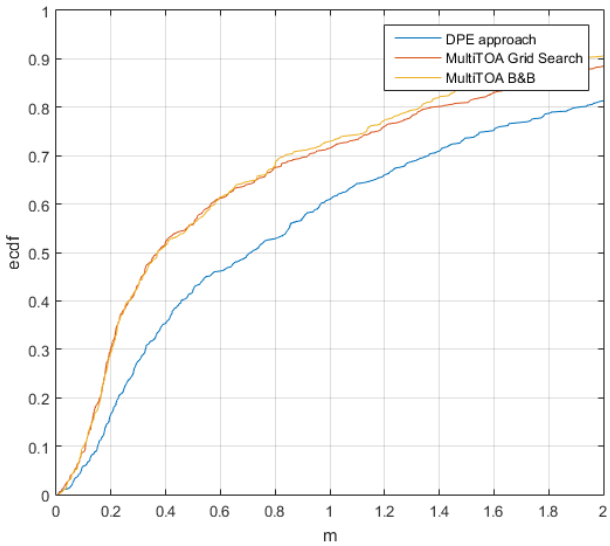

Fig. 35 Empirical cdf of the error for the DPE, MultiTOA B&B and GridSearch approach with 3 anchor nodes

However, in this case there is no such remarkable improvement with respect to the DPE approach. As we have mentioned in the previous section, when the number of anchors node is very low it may happen that 3 multipath components intersect more consistently than the path representing the true target. That's why we designed the MultiTOA weighted method.

4.3 MultiTOA Weighted

In the next simulation we will test the performance of the MultiTOA weighted algorithm using 3 anchors with a SNR at each anchor node of 4dB. The optimal parameter λ have been found empirically by running several simulations.

	RMSE
DPE	1.74m
MultiTOA B&B	1.23m
MultiTOA Weighted	0.22m

Table. 5 RMSE for MultiTOA Weighted approach with 3 anchor nodes

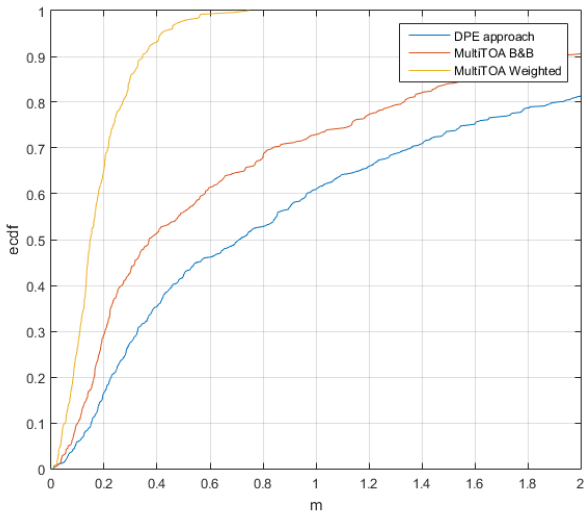

Fig. 36 Empirical cdf of the error for the DPE, MultiTOA and MultiTOA Weighted with 3 anchor nodes

We can state that the modifications in the MultiTOA algorithm lead to an important improvement. Using the same parameters as in the previous simulation we depict RMSE of the MultiTOA weighted against SNR:

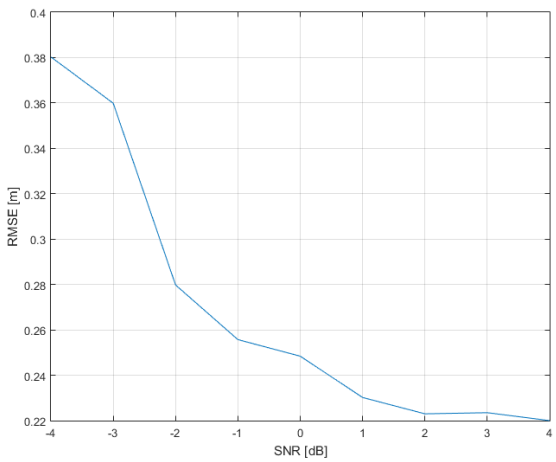

Fig. 37 RMSE vs SNR for the MultiTOA Weighted approach using 3 anchor nodes

From 4 to -2dB there is barely no decrease in performance and at -3dB the error starts to increase more prominently. However, even in these cases of low SNR, the proposed algorithm performs better than the DPE approach at high SNR conditions.

It is also important to highlight that in low SNR conditions the computational load of the algorithm increases. That's because the number of prominent peaks increases as the SNR decreases.

Finally, we will compare the performance of the two MultiTOA approach using 4 and 6 anchor nodes:

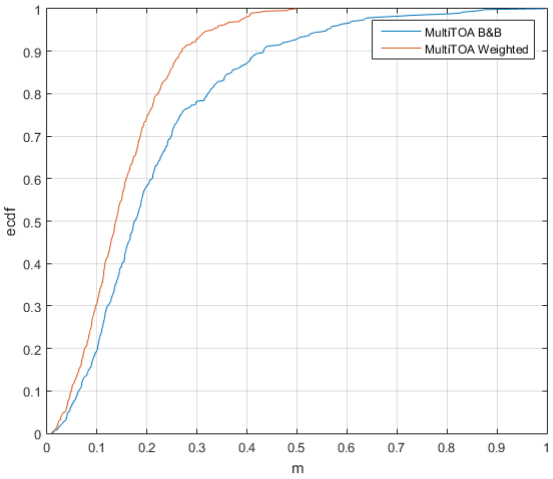

Fig. 38 Empirical cdf of the error for the MultiTOA and MultiTOA Weighted with 4 anchor nodes

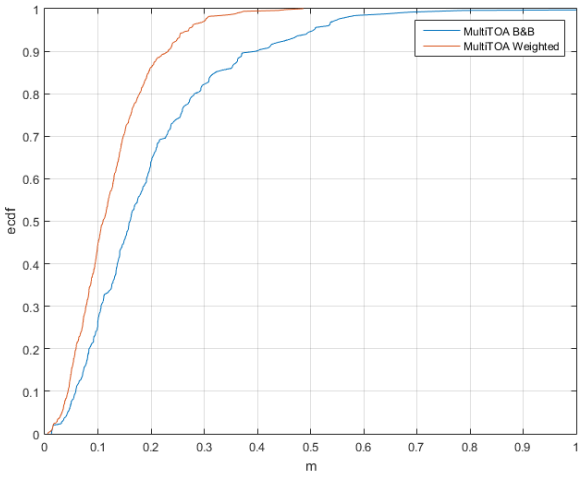

Fig. 39 Empirical cdf of the error for the MultiTOA and MultiTOA Weighted with 6 anchor nodes

	RMSE
MultiTOA B&B	0.27m
MultiTOA	0.18m

Table. 6 RMSE for MultiTOA Weighted approach with 4 anchor nodes

	RMSE
MultiTOA B&B	0.26m
MultiTOA	0.15m

Table. 7 RMSE for MultiTOA Weighted approach with 6 anchor nodes

In this case the improvement of the MultiTOA weighted with respect to the baseline MultiTOA is not so remarkable. That's because as the number of anchor nodes increases the probability of multipath components intersecting more consistently than the true path decreases.

All these simulations have been carried out without using compressive sensing. We refer the reader to the thesis developed by Ricard Garcia to see the performance of the algorithms presented in this thesis when applying compressive sensing.

7. Conclusions and future development:

In this thesis we have presented three new position estimation algorithms for UWB systems based on a frequency domain receiver that have been implemented and tested under the channel models provided in the standard IEEE 802.15.4a.

The results of the simulations show that the positioning techniques developed outperforms the base line DPE approach, providing then, robustness against the harsh characteristics of UWB channels which are its dense multipath and the strong attenuation of the direct-path or LOS. Apart from that, we can also claim that the proposed techniques are optimal in terms of computational load and moreover their performance holds for a wide range of SNR conditions.

Having this in mind, we can assure that the main aims of this project have been successfully achieved.

As future development of this thesis we could test the proposed algorithms under other UWB channels, such as the “Industrial LOS” CM7 which is also well-known for its dense multipath. Moreover, we could consider other inconveniences of UWB channels, such as Non-Line-of-Sight (NLOS) or Narrow Band Interference (NBI). It would also be interesting to study the optimal weighting criteria in a more formal and analytical way.

Bibliography:

[1] Navarro, Monica, and Montse Najar. "Frequency domain joint TOA and DOA estimation in IR-UWB." *IEEE transactions on wireless communications* 10.10 (2011): 1-11.

[2] Navarro, Monica, Pau Closas, and Montse Nájar. "Assessment of Direct Positioning for IR-UWB in IEEE 802.15. 4a channels." *2013 IEEE International Conference on Ultra-Wideband (ICUWB)*. IEEE, 2013.

[3] Lagunas, Eva, et al. "Spatial sparsity based direct positioning for IR-UWB in IEEE 802.15. 4a channels." *2014 IEEE International Conference on Ultra-WideBand (ICUWB)*. IEEE, 2014.

[4] Yang, Liuqing, and Georgios B. Giannakis. "Timing ultra-wideband signals with dirty templates." *IEEE Transactions on Communications* 53.11 (2005): 1952-1963.

[5] Dardari, Davide, Chia-Chin Chong, and Moe Win. "Threshold-based time-of-arrival estimators in UWB dense multipath channels." *IEEE Transactions on Communications* 56.8 (2008): 1366-1378.

[6] Li, Xinrong, and Kaveh Pahlavan. "Super-resolution TOA estimation with diversity for indoor geolocation." *IEEE Transactions on Wireless Communications* 3.1 (2004): 224-234.

[7] Gezici, Sinan, et al. "Localization via ultra-wideband radios: a look at positioning aspects for future sensor networks." *IEEE signal processing magazine* 22.4 (2005): 70-84.

[8] Lee, Joon-Yong, and Robert A. Scholtz. "Ranging in a dense multipath environment using an UWB radio link." *IEEE Journal on Selected Areas in Communications* 20.9 (2002): 1677-1683.

[9] Candès, Emmanuel J., and Michael B. Wakin. "An introduction to compressive sampling." *IEEE signal processing magazine* 25.2 (2008): 21-30.

[10] Rydstrom, Mats, Erik G. Strom, and Arne Svensson. "Robust sensor network positioning based on projections onto circular and hyperbolic convex sets (POCS)." *2006 IEEE 7th Workshop on Signal Processing Advances in Wireless Communications*. IEEE, 2006.

[11] Gholami, Mohammad Reza, et al. "Static positioning using UWB range measurements." *2010 Future Network & Mobile Summit*. IEEE, 2010.

[12] Arslan, Huseyin, Zhi Ning Chen, and Maria-Gabriella Di Benedetto, eds. *Ultra wideband wireless communication*. John Wiley & Sons, 2006.

[13] Di Benedetto, Maria-Gabriella, ed. *UWB communication systems: a comprehensive overview*. Vol. 5. Hindawi Publishing Corporation, 2006.

[14] Sahinoglu, Zafer, Sinan Gezici, and Ismail Guvenc. "Ultra-wideband positioning systems." *Cambridge, New York* (2008).

[15] Vaughan, Rodney G., and Neil L. Scott. "Super-resolution of pulsed multipath channels for delay spread characterization." *IEEE Transactions on Communications* 47.3 (1999): 343-347.

[16] Bellusci, Giovanni. Ultra-wideband ranging for low-complexity indoor positioning applications. TU Delft, Delft University of Technology, 2011.

[17] Molisch, Andreas F., et al. "IEEE 802.15. 4a channel model-final report." *IEEE P802* 15.04 (2004): 0662.

[18] Salman, Naveed, et al. "Effects of anchor placement on mean-CRB for localization." *Ad Hoc Networking Workshop (Med-Hoc-Net), 2011 The 10th IFIP Annual Mediterranean*. IEEE, 2011.

[19] Navarro, Monica, Simon Prior, and Montse Najar. "Low Complexity Frequency Domain TOA Estimation for IR-UWB Communications." *VTC Fall*. 2006.

8. Appendices:

1. Gantt diagram

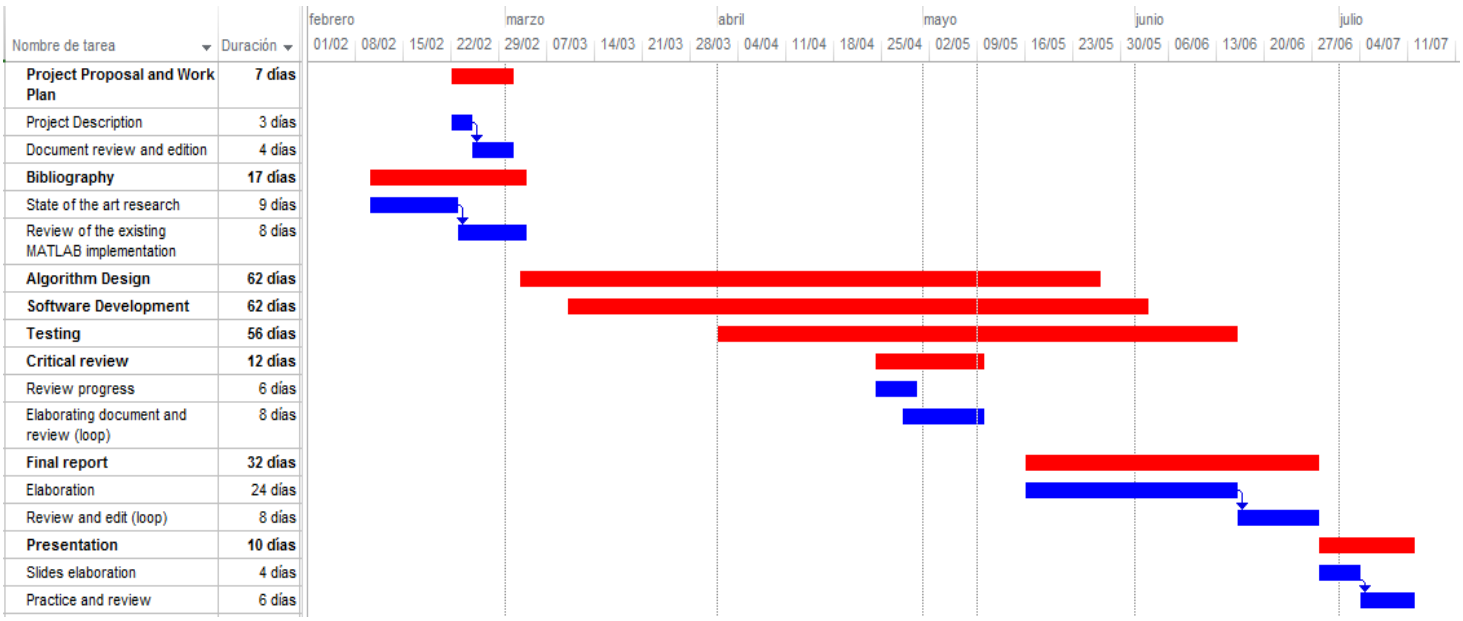

Nombre de tarea	Duración
Project Proposal and Work Plan	**7 días**
Project Description	3 días
Document review and edition	4 días
Bibliography	**17 días**
State of the art research	9 días
Review of the existing MATLAB implementation	8 días
Algorithm Design	**62 días**
Software Development	**62 días**
Testing	**56 días**
Critical review	**12 días**
Review progress	6 días
Elaborating document and review (loop)	8 días
Final report	**32 días**
Elaboration	24 días
Review and edit (loop)	8 días
Presentation	**10 días**
Slides elaboration	4 días
Practice and review	6 días